HHS Public Access

Author manuscript

J Orthop Res. Author manuscript; available in PMC 2016 October 01.

Published in final edited form as:

J Orthop Res. 2015 October ; 33(10): 1412–1423. doi:10.1002/jor.22944.

Genetic Loci that Regulate Ectopic Calcification in Response to Knee Trauma in LG/J by SM/J Advanced Intercross Mice

Muhammad Farooq Rai, Ph.D.[1,*], **Eric J. Schmidt, Ph.D.**[1,*], **Shingo Hashimoto, Ph.D.**[1], **James M. Cheverud, Ph.D.**[4], and **Linda J. Sandell, Ph.D.**[1,2,3]

[1]Department of Orthopaedic Surgery, Musculoskeletal Research Center, Washington University School of Medicine at Barnes-Jewish Hospital, 425 S. Euclid Avenue MS 8233, St. Louis, MO 63110, USA

[2]Department of Cell Biology and Physiology, Washington University School of Medicine at Barnes-Jewish Hospital, 425 S. Euclid Avenue MS 8233, St. Louis, MO 63110, USA

[3]Department of Biomedical Engineering, Washington University School of Medicine at Barnes-Jewish Hospital, 425 S. Euclid Avenue MS 8233, St. Louis, MO 63110, USA

[4]Department of Biology, Loyola University, 1050 W. Sheridan Road, Chicago, IL 60660, USA

Abstract

This study reports on genetic susceptibility to ectopic calcification in the LG/J and SM/J advanced intercross mice. Using 347 mice in 98 full-sibships, destabilization of medial meniscus (DMM) was performed to induce joint injury. We performed quantitative trait locus (QTL) analysis to map ectopic calcification phenotypes to discrete genomic locations. To validate the functional significance of the selected QTL candidate genes, we compared mRNA expression between parental LG/J and SM/J inbred strains. We found that joint destabilization instigated ectopic calcifications as detected and quantified by micro-CT. Overall, we detected 20 QTLs affecting synovial and meniscus calcification phenotypes with 11 QTLs linked to synovial calcification. Functional and bioinformatic analyses of single nucleotide polymorphism identified functional classifications relevant to angiogenesis (*Myo1e, Kif26b, Nprl3, Stab2, Fam105b*), bone

Corresponding author. Muhammad Farooq Rai, Ph.D., Department of Orthopaedic Surgery, Musculoskeletal Research Center, Washington University School of Medicine at Barnes-Jewish Hospital, 425 S. Euclid Avenue MS 8233, St. Louis, MO 63110 USA, Ph: 314-286-0955; Fax: 314-454-5900; raim@wudosis.wustl.edu.

*These authors contributed equally

Authors' contributions statement

All authors were involved in drafting and revision of the manuscript and all authors approved the final version to be published. Dr. Rai had full access to all of the data in the study and takes responsibility for the integrity of the data and the accuracy of the data analysis.

Study conception and design: Sandell, Rai, Cheverud

Acquisition of data: Rai, Schmidt, Hashimoto

Analysis and interpretation of data: Rai, Schmidt, Hashimoto, Sandell, Cheverud

Conflict of interest

Dr. Sandell is Editor in Chief of Journal of Orthopaedic Research. Dr. Sandell owns stock or stock options in ISTO Technologies and receives royalties from Merck/Millipore for a type IIA collagen N-propeptide enzyme-linked immunosorbent assay. All other authors have nothing to disclose. None of the authors has any competing interests with regard to this manuscript.

DATA SUBMISSION

Gene expression profiles of the samples have been deposited into the National Center of Biotechnology Information Gene Expression Omnibus (GEO, (http://www.ncbi.nlm.nih.gov/projects/geo) repository and are accessible through GEO series accession number GSE64793.

metabolism/calcification (*Tle3, Tgfb2, Lipc, Nfe2l1, Ank, Fam105b*), arthritis (*Stab2, Tbx21, Map4k4, Hoxb9, Larp6, Col1a2, Adam10, Timp3, Nfe2l1, Trpm3*), and ankylosing-spondylitis (*Ank, Pon1, Il1r2, Tbkbp1*) indicating that ectopic calcification involves multiple mechanisms. Furthermore, the expression of 11 candidate genes was significantly different between LG/J and SM/J. Correlation analysis showed that *Aff3*, *Fam81a*, *Syn3*, and *Ank* were correlated with synovial calcification. Taken together, our findings of multiple genetic loci suggest the involvement of multiple genes contributing to ectopic calcification.

Keywords

ectopic calcification; QTL analysis; gene expression; genetics; advanced intercross line; osteoarthritis

INTRODUCTION

Pathological mineralization of synovial connective tissues leads to chondromatosis or “loose bodies” in the knee[1; 2]. Ectopic nodules appear as multiple intra-articular calcifications[1; 3]. Their rupture and detachment can disturb the nutritive supply to the joint and can result in mechanical injury ultimately leading to osteoarthritis (OA)[3; 4].

Tissue mineralization is a complex phenomenon involving many physiological processes. Normally, bones, teeth, and otoconia are the principal mineralized human tissues while non-mineralized soft tissues are constantly awash in interstitial fluids supersaturated with calcium and phosphate with mineralization inhibited[5]. Disturbance of inhibitory mechanisms may permit pathological mineralization, e.g., atherosclerosis[6], renal calculus and gout[7; 8], skin ossifications[9], craniosynostosis[10], and OA-related ectopic calcification of joints. Some evidence suggests that synovial chondromatosis has a genetically simple or Mendelian basis[11; 12]. Segregation has been reported in several pedigrees[13], while casual loci have been mapped to human chromosomes 5p[11] and 8q[12]. A monogenic cause for ectopic calcification has been shown to be due to a segregating dominant allele of *ANK* on chromosome 5[14]. However, many cases appear to have a multifactorial basis. While it is likely that environmental components of risk are substantial, recurrence rate among first-degree relatives is 10–30%[15], indicative of genetic components. Constituting the majority of cases, genetic locations contributing to this polygenic form are unknown, let alone the physiological processes the gene variants affect. Identification of important susceptibility loci has highlighted disturbed physiological processes leading to calcification of joints and other tissues such as heterotrophic mineralization of musculoskeletal tissues, skin and blood vessels[6; 9].

Here, we report the development of synovial and meniscal ectopic calcifications in response to knee trauma in an F_{44} advanced intercross of LG/J and SM/J mice (Wustl:LG, SM-G44). We mapped synovial and meniscal ectopic calcification phenotypes to discrete genomic locations. For each positional candidate gene, we compared genetic sequence variations between LG/J and SM/J alleles and performed functional, bioinformatic, and expression analyses to gain insight into the mechanisms underlying these phenotypes.

MATERIALS AND METHODS

Mice and knee injury model

All experiments were approved by the Animal Studies Committee. The F_{44} advanced intercross differs in a wide-range of traits and is a model for studying the genetics of complex traits segregating many interacting genes of small effect[16–19]. The F_{44} sample included 347 mice in 98 full-sibships. All mice were raised at our mouse facility operating at constant temperature of 21°C and on a 12-hour light/dark cycle at high standards of sanitation. Offspring were housed with their mothers until weaning at 3-weeks of age, and then separated into sex-specific cages of 4–5 mice/cage with each cage individually ventilated. All mice were fed on irradiated rodent chow (Purina 5053, Purina Mills St. Louis, MO) with food and water provided *ad libitum*.

OA was induced through DMM surgery in which the medial meniscotibial ligament (MMTL) was transected in 10-week old mice as described by us[20] and others[21]. Mice were anesthetized using an intra-peritoneal injection of rodent cocktail (100 mg/kg ketamine, 20 mg/kg xylazine and 10 mg/kg acepromazine) before their right knee MMTL was resected to displace the medial meniscus. The contralateral left knee served as a sham, receiving the exact same surgery as DMM but without severing the MMTL. The primary reason for using the contralateral sham knee in these experiments is because we are using F44 generation families and the control knee must have exactly the same genotype as the DMM knee. Mice were sacrificed by CO_2 asphyxiation at indicated time points. Knees were harvested and subjected to histological and micro-CT analyses. After surgery, mice were transferred to their original cages with original inmates in a group of 4–5 mice. All mice were weight bearing after 2 hours when they recovered from anesthesia. No running wheels or casts were provided therefore all the mice experienced equal levels of activity. All surgeries were performed by one surgeon.

Micro-CT analysis and phenotypic scoring

Ectopic calcifications were visualized by micro-computed tomography (micro-CT) scanner (Scanco-Medical) as described previously[20]. Each mouse was scored for presence/absence of synovial and/or meniscal ectopic calcifications as well as according to a graded scale: 0 = no nodules, 1 = <5 nodules, 2 = ≥5 nodules (Fig 1). We coded meniscal and synovial calcifications as separate phenotypes for the following reasons: The mouse meniscus is normally partially calcified, to a degree sufficient to render them visible on micro-CT. So, in this case, we are scoring the extent of normal calcification. The synovial tissue, on the other hand, is normally un-mineralized soft tissue. Hence it is quite possible that the two phenotypes are mechanistically unrelated, de novo calcification versus enhanced calcification. Further, measured phenotypes for meniscus calcifications and synovial calcifications are uncorrelated in a chi-square test of association (Cramer's V = 0.040, p = 0.905, 3 df); they are distributed as independent traits.

Histological analysis

Harvested knees were fixed overnight in 4% paraformaldehyde and methacrylate embedded. For proteoglycan detection, 10-um coronal sections were stained with Alcian blue and

Safranin-O, and counterstained with fast green. Mineralization was detected with 1% silver nitrate as per the von Kossa method. For immunohistochemistry of collagen types I and collagen type II, knees were fixed in 10% neutral buffered-formalin, decalcified with 10% formic acid in 5% formaldehyde for 48-hours, and embedded in paraffin. Coronal sections (5-um in thickness) were taken through the joint and evaluated for immunofluorescence as described elsewhere[22].

QTL mapping

Individuals of the F_{44} and their F_{43} parents were genotyped at 4,588 single nucleotide polymorphisms (SNPs) distributed across the 19 autosomes of the mouse genome[23]. A genetic map was constructed based on the physical ordering of SNPs along each autosome (Supplementary Table 1) according to NCBI build 37/mm9 (http://genome.ucsc.edu/) using R/qtl. Using the Hapi software[24], ordered heterozygous genotypes were estimated twice from family data. Heterozygous genotypes were input initially as “LG/J:SM/J” and then “SM/J LG/J”. Loci with discrepant calls between the two analyses were treated as having missing phase information.

Based on each individual’s marker genotypes, we utilized Haley-Knott regression[25] to impute additional genotypes every 1 centimorgan (cM), assigning additive, dominance, and imprinting genotypic scores at each marker and imputed position[18]. Then two mapping models were compared using the Mixed Procedure in SAS v9.1 (SAS Institute, Cary, NC). The full-model included sex plus genomic location effects and their interactions with sex as fixed effects, and family assignment and its interaction with sex as random effects. The −2 ln(likelihood) of the reduced and full-models were compared to a null-model including a sex effect but no specific genetic effect, using χ^2 test with 3 and 6 degrees-of-freedom, respectively. Probabilities were transformed into LPR = $-\log_{10}$(Pr). Bonferroni-adjusted genome-wise and chromosome-wise significance thresholds were calculated (Supplementary Table 1). Since meniscal and synovial calcifications were scored twice according to our binary and graded classifications, QTLs of a given full- or reduced-model were considered valid only when they achieved at least chromosome-wise significance on one scale and at least point-wise significance at 10% level on the other scale. For loci significant under the full mapping model and with interaction terms significant at the point-wise level (LPR≥1.3), the data were partitioned by sex and refitted to the reduced-model. We used the standard of a peak LPR score ±1 LPR to define 95% positional support intervals. When two QTLs for the same phenotype appeared on the same chromosome within 50 cM of each other, the two positions were considered individually and jointly. A 2-QTL model was accepted if it fitted better at 5% significance than the best 1-QTL model using a likelihood ratio test.

SNP analysis

Using UCSC genome browser annotations of the NCBI37/mm9 assembly (http://genome.ucsc.edu/), we identified SNPs in the exons, introns, and untranslated regions of each candidate. SNPs occurring within 2500 base-pairs up- and down-stream of transcription start and stop sites were considered. Evolutionary conservation scores for each SNP were obtained from the PhastCons30Placental table (UCSC browser). Nonsynonymous SNPs

were evaluated for potential functional significance by PolyPhen-2, SIFT, and LRT algorithms[19; 26–29].

Candidate genes and functional classifications

We analyzed candidate genes by GeneGo MetaCore (https://portal.genego.com) to assess the gene ontology. We then performed a PubMed search for each candidate using its name plus these terms joined by the Boolean operator OR: arthritis, bone, calcification, cartilage, mineralization, osteocyte, synovium. Search results were perused for relevance to OA processes or skeletal tissue physiology. Further information regarding the molecular function, cellular component, and biological process were probed using Mouse Genome Informatics (MGI) gene ontology database (http://www.informatics.jax.org). We also used gene expression omnibus (http://www.ncbi.nlm.nih.gov/geo) to search for mutant alleles of our positional candidates with effects on skeletal tissues and to examine information regarding their expression patterns.

Enrichment ankylosing spondylitis-associated genes

We tested whether our QTL support intervals were enriched for candidates with human orthologs associated with ankylosing spondylitis. We compiled a list of 213 genes associated with ankylosing spondylitis using the Genotator database (http://www.genotator.hms.harvard.edu/geno). For each actual QTL detected, we positioned a support interval of equal size randomly in the mouse genome without resampling positions, counting the number of genes within intervals that occur on the disease association list. The process was repeated 1,000 times to arrive at the expected number of such occurrences.

Validation of candidate genes in parental LG/J and SM/J inbred strains

To validate the functional significance of the selected QTL candidate genes, we set out to compare mRNA expression levels in knee joint tissues between parental LG/J and SM/J inbred strains for 78 candidate genes. Using five mice from each parental strain, we performed DMM in the right knees as described above. At 8-week post-surgery, knees were harvested and scanned to evaluate ectopic calcification by the aforementioned micro-CT analysis. The knee joints were fixed in 10% neutral buffered formalin and decalcified using a mixture of 10% formic acid and 5% formaldehyde solution for 2-days at 4°C. Then the joints were incubated in 0.01 M ethylenediaminetetraacetic acid for another 6 hours at room temperature. Samples were paraffin embedded, mounted in blocks, and sagittally sectioned at 5 μm intervals using standard methods. The sections were mounted on polylysine-coated slides (Fisher Scientific, Silver Spring, MD) before staining. We used the Affymetrix QuantiGene Plex assay (Panomics Inc., Fremont, CA) to measure the mRNA expression in tissue lysate prepared from formalin-fixed paraffin embedded histological sections[29]. Briefly, 25 sections of sham- and DMM-operated knees were macrodissected to collect the entirety of the knee capsule tissues including subchondral bone of the tibia and femur, while removing excess paraffin and extraneous long bone material, prior to tissue homogenization. Tissue homogenates were prepared in a mixture of homogenizing solution and proteinase K. The mRNA expression of candidate genes was measured in tissue lysates by the Affymetrix QuantiGene Plex assay (Panomics Inc., Fremont, CA) as described previously[29]. The expression of candidate genes was normalized by obtaining their residuals from a multiple

regression using *Gapdh* and *Hprt1* readings as independent variables. Residuals from replicates were then averaged to obtain normalized readings from each knee per individual mouse. LG/J and SM/J gene expression levels were compared using correlated t-tests in which the expression level of the sham-operated knee was subtracted from the DMM-knee of each individual. We also computed the Pearson's correlation coefficients between ectopic calcification scores and levels of gene expression for those candidate genes whose expression levels were significantly different between LG/J and SM/J at the ≤10% level of significance.

RESULTS

Phenotypic analysis

Ectopic nodules were analyzed at 8-weeks post-injury. Micro-CT analysis revealed calcified nodules around joint capsule, synovium, or meniscus only in the knees that underwent DMM surgery (Fig. 2B and 2D). No nodules were present in sham-operated knees (Fig. 2A and 2C). It was shown that LG/J mouse strain developed significantly more ectopic calcification in the right operated knee compared to contralateral left sham-operated knee as well as when compared to the DMM-operated knee of SM/J mouse strain (Fig. 2E and 2F). Our histological analysis confirmed the mineralized nature of ectopic nodules as was evident by von Kossa staining (Fig. 3A–B). These nodules stained positively for Alcian blue and Safranin-O, indicating abundant expression of glycosaminoglycan substituted proteoglycan components (Fig. 3C–D) of the type primarily present in cartilage along with collagen type II expression (Fig. 3E). These regions also stained positively for both collagen types I and II (Fig. 3F). The medial joint capsule of DMM-treated knees showed hypertrophy and expressed higher type II collagen compared to sham. Type II collagen expression was predominately on the periphery of the nodules while type I collagen was expressed mainly in the center.

QTL analysis

Overall, we detected 20 QTLs affecting synovial and meniscal calcification phenotypes with 11 QTLs linked to synovial calcification and 10 QTLs affecting meniscal calcification (Table 1). Calcification QTLs are identified by *C* followed by two numbers separated by a decimal. The first number indicates QTL's chromosome; the second number identifies particular QTLs on the same chromosome. Mouse chromosomes are acrocentric, and QTLs on the same chromosome are numbered according to their relative position from the centromere. Among all the QTLs, only *C19.1* exerted a pleiotropic effect on both phenotypes. While all other QTLs attained at least chromosome-wise significance, *C1.2* affecting synovium achieved genome-wise significance with an LPR≥4.35. In contrast, *C8.1* was only tentatively accepted since it occurred in a proximal region on chromosome 8 in which SM/J alleles were infrequent after 44 generations of genetic drift; so genotypic means for homozygotes at this locus were estimated from very few individuals.

Sex effects were important, with 13 loci demonstrating significantly different effect sizes dependent on sex. An additive effect is half the difference between the means calcification scores of the two homozygotes. To compare effect sizes across phenotypes, we standardized

them by dividing by their respective standard deviations (SD) obtained via one-way analysis of variance with sex as the independent factor. LG/J at *C1.1* conferred the largest additive protective effect with a/SD = −1.223. This effect was only significant in males and was the largest overall effect. *C5.1* conferred the largest additive increase in susceptibility with a/SD = 0.589 and affected both sexes equally. Among homozygotes at *C8.1*, the LG/J allele protected males (a/SD = −0.625) but increased ectopic calcifications in females (a/SD = 0.331). Of 14 significant additive effects, the LG/J allele was found to be protective against developing ectopic calcification at eight QTLs and susceptible to it at six locations (Table 1).

We detected 13 significant dominance effects (describing the difference between calcification score of heterozygotes and homozygotes), 10 of which reduced calcification scores indicating the general dominance of protective alleles. The largest reduction of susceptibility was conferred on males by *C1.2* with d/SD = −0.502. In terms of dominance, females were most susceptible at *C1.6* (d/SD = 0.893). Males were protected at *C10.1* (d/SD = −0.469), while females were more prone to develop ectopic calcifications (d/SD = 0.345).

Given our experimental design, we were able to investigate imprinting effects at heterozygous loci, which measured phenotypic differences between heterozygotes receiving their LG/J and SM/J alleles from parents of opposite sex. We observed 10 cases of significant imprinting, similar in number to additive and dominance effects that are more commonly tested in genetic studies. Inheriting the LG/J allele from the dam reduced susceptibility in six of 10 cases of significant imprinting, most notably for males at *C14.1* (i/SD = −0.460). At *C1.3*, inheriting LG/J from the sire protected females (i/SD = −0.334) but made males more susceptible (i/SD = 0.511).

Candidate gene nomination and prioritization

The average QTL support interval size was 1.15 megabases, containing on average seven or eight genes in the F_{44} advanced intercross line. From 141 positional candidates clustered in 20 QTL regions (Supplementary Table 2), we compiled two lists of priority candidate genes. An initial list of 35 candidates was determined through bibliographic searches to be associated with normal or disease states affecting skeletal tissues or to be involved in ectopic mineralization of soft tissues. A second list of 66 candidates was based on genes containing non-synonymous SNPs and/or highly conserved SNPs at noncoding positions (Table 2). Of these, 25 candidates harbored nonsynonymous SNPs and were further scrutinized using predictive algorithms for the likelihood that the resulting amino acid changes have functional consequences. The following genes contained the greatest number of coding SNPs in their respective QTL intervals: *Aff3* (*C1.1*), *Il1rl2* (*C1.2*), *Zfp648* (*C1.3*), *Rrp15* (*C1.5*), *Hip1* (*C5.2*), *Uaca* (*C9.1*), *Stab2* (*C10.1*), *Oxgr1* (C*14.1*), *Fam105a* (*C15.1*), and *Sorcs1* (*C19.1*) (Table 2; Supplementary Table 3). *Stab2*, *Oxgr1*, and *Fam105a* were predicted by either LRT, PolyPhen-2, and/or SIFT algorithms as encoding amino-acid polymorphisms of likely functional consequence, and as such were among the most highly ranked candidates. *Il1rl2* and *Stab2* are also distinguished by carrying numerous nonsynonymous SNPs, six and 14, respectively. MGI databases indicated that *Aff3* is expressed in the axial skeleton, with one known mutant producing malformed vertebrae. Similarly, one mutant form of *Hip1* caused axial malformations but yielded no specific arthritic phenotypes in joints of the appendicular

skeleton. Of the other nonsynonymous SNP-carrying candidates, very little information is available regarding expression and functional roles in skeletal tissues. Fifty-eight genes from our list of 66 candidates contained only highly conserved noncoding SNPs. According to the MGI database, *Rasl11b* is expressed in pelvic skeletal tissue, *Pon1* and *Pon2* are expressed in the femur, and *Gmds* is expressed in appendicular skeleton. QTL interval *C4.1* contained no known genes, and its phenotypic effects were likely due to regulatory sequences.

Ankylosing spondylitis-associated gene enrichment

From our QTL analysis, we found that four candidate genes have human orthologs that are associated with ankylosing spondylitis (*Ank, Pon1, Il1r2, Tbkbp1*). From our simulation described above, we expect to observe on average 1.66 such genes by random chance. The non-parametric probability of the result is P = 0.059, suggesting that whatever processes underlie ankylosing-spondylitis in human are likely important in ectopic calcification in our mouse model of knee injury.

Gene expression differences between parental LG/J and SM/J inbred strains

We observed that the expression levels of 11 candidate genes were significantly different between LG/J and SM/J mice at the 10% level or lower: *Aff3* (P = 0.03), *Gpatch2* (P = 0.07), *Pon2* (P = 0.06), *Uaca* (P = 0.10), *Fam81a* (P = 0.02), *Syn3* (P = 0.03), *Copz2* (P = 0.07), *Skap1* (P = 0.03), *Mrpl10* (P = 0.04), *Nfe2l1* (P = 0.05) and *Ank* (P = 0.09) (Table 3). Correlation analysis showed that *Aff3* (r = 0.56; P = 0.02), *Fam81a* (r = 0.46; P = 0.06), *Syn3* (r = 0.43; P = 0.08), and *Ank* (r = 0.40, P = 0.10) were correlated with synovial calcification phenotype.

DISCUSSION

We performed genome-wide mapping of QTLs affecting synovial and meniscus calcifications in an F_{44} advanced intercross line derived from LG/J and SM/J mice. We mapped 20 QTLs in our experimental population affecting ectopic calcification with 11 and 10 QTLs respectively underlying synovial and meniscal calcifications. The LG/J allele usually conferred an increased protective effect against ectopic calcification relative to the SM/J allele. Sex-specific genetic effects predominated, with 13 loci demonstrating significantly different effect sizes dependent on sex. At the expense of detection power, advanced intercross lines provided a mapping advantage over F_2 or backcross generations in that QTL numbers and locations are more precisely localized. The average interval size was 1.15 megabases, typically containing 7–8 genes. We discuss candidate genes in terms of functional classifications encompassing angiogenesis, bone metabolism, calcification, arthritis, and ankylosing spondylitis.

Angiogenesis

Several genes associated with angiogenesis were identified in our QTLs intervals (*Myo1e, Kif26b, Nprl3, Stab2, Fam105b*). Angiogenesis is associated with ectopic calcification in a variety of tissues[30] and exerts both direct and indirect effects on ectopic calcification through a two-step process: firstly, angiogenic factors and cytokines released by endothelial cells induce the differentiation of osteogenic progenitor cells and secondly, blood vessels

provide oxygen and nutrients to initiate and augment bone growth[31]. While chondrocalcinosis is not always associated with increased angiogenesis[32], it is believed that synovial and osteochondral angiogenesis are both features of arthritis and occur in parallel.

Bone metabolism and calcification

Deposition of calcium crystals in cartilage and meniscus is often associated with higher risk of OA[33]. Calcium crystals with a low propensity to induce acute inflammation may contribute to chronic synovitis and angiogenesis in chondrocalcinosis.

Tle3 (*C9.1*) varied at two highly conserved intronic SNPs, and is known to be involved in osteoblast differentiation[34]. Likewise, *Tgfb2* (*C1.5*) is known to play significant roles in bone metabolism and turnover[35], though alleles did not vary at evolutionarily conserved sites. While *Lipc (C9.2)* is expressed in osteocytes, and is associated with bone mineral density variation and coronary calcification[36], it harbored no highly conserved SNPs. *Nfe2l1 (C11.1)*, which contained six conserved noncoding SNPs, plays a role in bone development[37].

Ankylosing spondylitis

In our study, *ANK*, which is associated with synovial chondromatosis in humans, was linked to meniscus calcification at *C15.1*. Finding *Ank* in an interval is very intriguing, yet according to our SNP criteria, it is outranked by *Fam105b* (associated with angiogenesis as above), a gene about which little is known but among our most highly ranked candidates based on SNP polymorphisms. Nonetheless, *Ank* plays an important role in inorganic pyrophosphate transport and inhibition of matrix mineralization[38], and its human variants have been associated with joint chondrocalcinosis and ankylosing spondylitis[39].

Interestingly, in addition to *Ank*, we found three other candidates (*Pon1*, *Il1r2*, and *Tbkbp1*) associated with human ankylosing spondylitis[40], OA and RA[41]. Members of the *IL1* gene cluster also play roles in growth plate and bone remodeling[42]. We noted for *Il1r2* and *Tbkbp1*, and more generally for other candidates lacking conserved and/or nonsynonymous SNPs, that we defined alleles to include transcribed sequences plus the flanking 2,500 base-pairs linked but more distant regulatory sequences remain unexplored.

Arthritis

Though we did not find bibliographic evidence for its association with OA phenotypes, *Stab2* (*C10.1*) binds to hyaluronic acid in the extracellular matrix[43]. Between the LG/J and SM/J, *Stab2* varied at 14 nonsynonymous positions. *Tbx21 (C11.1)*, differing at two highly conserved intronic SNPs, plays a role in T-cell function underlying numerous autoimmune disorders including rheumatoid arthritis (RA) and systemic sclerosis[44]. *Map4k4 (C1.3)* contained six highly conserved intronic SNPs, and human variants have been associated with RA and arterial calcification[45]. *Hoxb9* (*C11.1*) is associates with human hip dysplasia and OA[46] and varied at two conserved intronic and three downstream base positions. *Larp6* (*C9.1*) functions in large part by directly binding to *Col1a2* during its translation[47], however, both *Col1a2 (C6.1) and Larp6* carried no significant SNPs. In contrast, *Adam10* (*C9.2,*) a member of aggrecanase family involved in proteolytic cleavage of protein ectodomains

including those of Notch receptors[48], as well as aggrecan varied at a single conserved intronic position. A role for metalloproteases was further implied by *C10.1* candidate *Timp3*, containing four conserved intronic SNPs, which interacts with metalloproteases[49] and plays a key role in inflammation and OA[50]. Playing a role in normal bone development, *Nfe2l1* (*C11.1*) contains six conserved noncoding SNPs. In humans, *NFE2l1* is an important transcription factor implicated in the regulation of genes differentially expressed between normal and RA patients[41]. *Trpm3* is a calcium permeable channel associated with human RA through dysregulated synoviocyte secretion of hyaluronic acid[51]. It has one nonsynonymous SNP in addition to 32 highly conserved intronic SNPs.

Despite the fact that several genes identified from calcification phenotype to be associated with OA, to our knowledge, no QTL for OA in the mouse model have been reported other than a single locus found in STR/ort mice[52], the main candidate being Sfrp1, a WNT antagonist. This QTL is located on chromosome 4 in a region distinct from our QTL on chromosome 4, C4.1.

To further address the functional relevance of candidate genes underlying post-traumatic ectopic calcification, we measured calcification phenotypes and expression levels of several candidate genes in the advance intercross parental strains, LG/J and SM/J. Our mRNA expression analysis showed that the expression of 11 candidates was significantly different between LG/J and SM/J, with four being correlated with the degree of ectopic calcification. Given the predominant effect of sex in our analyses, we suggest future mechanistics studies should have an explicit focus on the role of sex in modulating biological processes underlying ectopic calcification. Thus, continuing this approach coupled with mechanistic studies will further narrow the scope of our candidate genes toward the aim of identifying precise physiological mechanisms underlying ectopic calcification of joints following traumatic knee injury.

Our findings of multiple genetic loci affecting ectopic calcification suggest the involvement of multiple genes contributing to its pathogenesis. Our data also suggest pathogenic mechanisms leading to post-traumatic calcification in the joint space versus the synovium have distinct and overlapping components. As mentioned above, we coded meniscal and synovial calcifications as separate phenotypes because they are mechanistically unrelated: de novo calcification in one versus enhanced calcification in the other. In addition, these phenotypes were found to be uncorrelated in a chi-square test of association. Considering the distinct nature of these two tissue environments as well as the outcome from statistical test, we coded meniscus and synovial calcifications as distinct phenotypes yielding a total of 20 QTL loci. We considered the possibility that the calcifications should be coded as a single phenotype but their lack of phenotypic correlation and their distinct normal and pathological states led us to treat them separately.

Lastly, we believe the present analysis to be the first detailed genetic examination of meniscal or synovial calcification phenotypes resulting from knee-trauma in mice. We are not aware of any studies that have examined these meniscal or synovial calcification phenotypes in other mouse strains. However, we strongly believe that DMM surgery per se is not the sole inducer of these phenotypes as our unpublished observations in some of the

genetic mouse strains have shown that non-invasive compressive loading also results in the formation of calcified nodules in the synovium and meniscus (MF Rai, D. Xin, LJ Sandell, unpublished results. We have previously reported that certain LGXSM recombinant inbred lines capable of healing ear wounds and repairing articular cartilage defects are protected against induced knee OA[2022]. Interestingly, the healer mice develop higher degree of ectopic calcification than a mouse strain that does not repair above tissues and is susceptible to post-traumatic osteoarthritis. Therefore, we suggest that formation of ectopic calcification is an independent phenomenon and does not depend on the status of articular cartilage. Taken together with the lack of effect of sham surgery, we interpret our experimental analysis to reflect the calcifying response of the murine knee to generalized trauma and specifically here to joint instability caused by meniscal destabilization.

Supplementary Material

Refer to Web version on PubMed Central for supplementary material.

Acknowledgments

These studies were supported by an R01AR063757 (Sandell, Cheverud) and by P30-AR057235 (Musculoskeletal Research Center, Sandell, P.I.) from the National Institute of Arthritis, Musculoskeletal and Skin Diseases (NIAMS). Dr. Rai is supported through NIH Pathway to Independence Award (1K99AR064837) from NIAMS. Dr. Schmidt is supported through NIH T32 Metabolic Skeletal Disorders Training program (T32-AR-060719) from NIAMS. The content of this publication is solely the responsibility of the authors and does not necessarily represent the official views of the NIH or the NIAMS. We acknowledge with thanks Dr. Amy Williams (Massachusetts Institute of Technology, Cambridge, MA) for providing us with an advanced version of the minimum recombination option (hapi-mr) of the Hapi program, enabling us to phase our larger mouse families comprising up to 16 offspring. We also acknowledge with thanks the important technical support by Crystal Idleburg and Kara Janiszak.

REFERENCES

1. Crotty JM, Monu JU, Pope TL Jr. Synovial osteochondromatosis. Radiologic clinics of North America. 1996; 34:327–342. xi. [PubMed: 8633119]
2. Barwell R. Clinical Lectures on Movable Bodies in Joints. Br Med J. 1876; 1:184–185.
3. Felson DT, Anderson JJ, Naimark A, et al. The prevalence of chondrocalcinosis in the elderly and its association with knee osteoarthritis: the Framingham Study. J Rheumatol. 1989; 16:1241–1245. [PubMed: 2810282]
4. Wilkins E, Dieppe P, Maddison P, et al. Osteoarthritis and articular chondrocalcinosis in the elderly. Ann Rheum Dis. 1983; 42:280–284. [PubMed: 6859960]
5. Steitz SA, Speer MY, McKee MD, et al. Osteopontin inhibits mineral deposition and promotes regression of ectopic calcification. Am J Pathol. 2002; 161:2035–2046. [PubMed: 12466120]
6. Ji Y, Christopherson GT, Kluk MW, et al. Heterotopic ossification following musculoskeletal trauma: modeling stem and progenitor cells in their microenvironment. Adv Exp Med Biol. 2011; 720:39–50. [PubMed: 21901617]
7. Ciancio G, Bortoluzzi A, Govoni M. Epidemiology of gout and chondrocalcinosis. Reumatismo. 2011; 63:207–220. [PubMed: 22303527]
8. Moochhala SH. Extracellular pyrophosphate in the kidney: how does it get there and what does it do? Nephron Physiology. 2012; 120:33–38.
9. Li Q, Uitto J. Mineralization/anti-mineralization networks in the skin and vascular connective tissues. Am J Pathol. 2013; 183:10–18. [PubMed: 23665350]
10. Richtsmeier JT, Flaherty K. Hand in glove: brain and skull in development and dysmorphogenesis. Acta neuropathologica. 2013; 125:469–489. [PubMed: 23525521]

11. Hughes AE, McGibbon D, Woodward E, et al. Localisation of a gene for chondrocalcinosis to chromosome 5p. Hum Mol Genet. 1995; 4:1225–1228. [PubMed: 8528213]
12. Baldwin CT, Farrer LA, Adair R, et al. Linkage of early-onset osteoarthritis and chondrocalcinosis to human chromosome 8q. Am J Hum Genet. 1995; 56:692–697. [PubMed: 7887424]
13. Rodriguez-Valverde V, Zuniga M, Casanueva B, et al. Hereditary articular chondrocalcinosis. Clinical and genetic features in 13 pedigrees. Am J Med. 1988; 84:101–106. [PubMed: 3422129]
14. Pendleton A, Johnson MD, Hughes A, et al. Mutations in ANKH cause chondrocalcinosis. Am J Hum Genet. 2002; 71:933–940. [PubMed: 12297987]
15. Balsa A, Martin-Mola E, Gonzalez T, et al. Familial articular chondrocalcinosis in Spain. Ann Rheum Dis. 1990; 49:531–535. [PubMed: 2383079]
16. Hrbek T, de Brito RA, Wang B, et al. Genetic characterization of a new set of recombinant inbred lines (LGXSM) formed from the inter-cross of SM/J and LG/J inbred mouse strains. Mamm Genome. 2006; 17:417–429. [PubMed: 16688532]
17. Cheverud JM, Routman EJ, Duarte FA, et al. Quantitative trait loci for murine growth. Genetics. 1996; 142:1305–1319. [PubMed: 8846907]
18. Cheverud JM, Lawson HA, Fawcett GL, et al. Diet-dependent genetic and genomic imprinting effects on obesity in mice. Obesity (Silver Spring). 2011; 19:160–170. [PubMed: 20539295]
19. Cheverud JM, Lawson HA, Bouckaert K, et al. Fine-mapping quantitative trait loci affecting murine external ear tissue regeneration in the LG/J by SM/J advanced intercross line. Heredity (Edinb). 2014; 112:508–518. [PubMed: 24569637]
20. Hashimoto S, Rai MF, Janiszak KL, et al. Cartilage and bone changes during development of post-traumatic osteoarthritis in selected LGXSM recombinant inbred mice. Osteoarthritis Cartilage. 2012; 20:562–571. [PubMed: 22361237]
21. Glasson SS, Blanchet TJ, Morris EA. The surgical destabilization of the medial meniscus (DMM) model of osteoarthritis in the 129/SvEv mouse. Osteoarthritis Cartilage. 2007; 15:1061–1069. [PubMed: 17470400]
22. Rai MF, Hashimoto S, Johnson EE, et al. Heritability of articular cartilage regeneration and its association with ear wound healing in mice. Arthritis Rheum. 2012; 64:2300–2310. [PubMed: 22275233]
23. Lawson HA, Cady JE, Partridge C, et al. Genetic effects at pleiotropic loci are context-dependent with consequences for the maintenance of genetic variation in populations. PLoS Genet. 2011; 7:e1002256. [PubMed: 21931559]
24. Williams AL, Housman DE, Rinard MC, et al. Rapid haplotype inference for nuclear families. Genome biology. 2010; 11:R108. [PubMed: 21034477]
25. Haley CS, Knott SA. A simple regression method for mapping quantitative trait loci in line crosses using flanking markers. Heredity (Edinb). 1992; 69:315–324. [PubMed: 16718932]
26. Kumar P, Henikoff S, Ng PC. Predicting the effects of coding non-synonymous variants on protein function using the SIFT algorithm. Nature protocols. 2009; 4:1073–1081. [PubMed: 19561590]
27. Adzhubei IA, Schmidt S, Peshkin L, et al. A method and server for predicting damaging missense mutations. Nature methods. 2010; 7:248–249. [PubMed: 20354512]
28. Chun S, Fay JC. Identification of deleterious mutations within three human genomes. Genome Res. 2009; 19:1553–1561. [PubMed: 19602639]
29. Rai MF, Schmidt EJ, McAlinden A, et al. Molecular insight into the association between cartilage regeneration and ear wound healing in genetic mouse models: targeting new genes in regeneration. 2013; G3(3):1881–1891.
30. Ronchetti I, Boraldi F, Annovi G, et al. Fibroblast involvement in soft connective tissue calcification. Frontiers in genetics. 2013; 4:22. [PubMed: 23467434]
31. Collett GD, Canfield AE. Angiogenesis and pericytes in the initiation of ectopic calcification. Circ Res. 2005; 96:930–938. [PubMed: 15890980]
32. Piovesan EJ, Young Blood MR, Kowacs PA, et al. Prevalence of migraine in Noonan syndrome. Cephalalgia : an international journal of headache. 2007; 27:330–335. [PubMed: 17376109]

33. Neame RL, Carr AJ, Muir K, et al. UK community prevalence of knee chondrocalcinosis: evidence that correlation with osteoarthritis is through a shared association with osteophyte. Ann Rheum Dis. 2003; 62:513–518. [PubMed: 12759286]
34. Kokabu S, Nguyen T, Ohte S, et al. TLE3, transducing-like enhancer of split 3, suppresses osteoblast differentiation of bone marrow stromal cells. Biochem Biophys Res Commun. 2013; 438:205–210. [PubMed: 23880346]
35. Filvaroff E, Erlebacher A, Ye J, et al. Inhibition of TGF-beta receptor signaling in osteoblasts leads to decreased bone remodeling and increased trabecular bone mass. Development. 1999; 126:4267–4279. [PubMed: 10477295]
36. Yamada Y, Ando F, Shimokata H. Association of candidate gene polymorphisms with bone mineral density in community-dwelling Japanese women and men. Int J Mol Med. 2007; 19:791–801. [PubMed: 17390085]
37. Kim J, Xing W, Wergedal J, et al. Targeted disruption of nuclear factor erythroid-derived 2-like 1 in osteoblasts reduces bone size and bone formation in mice. Physiol Genomics. 2010; 40:100–110. [PubMed: 19887580]
38. Gurley KA, Reimer RJ, Kingsley DM. Biochemical and genetic analysis of ANK in arthritis and bone disease. Am J Hum Genet. 2006; 79:1017–1029. [PubMed: 17186460]
39. Pimentel-Santos FM, Ligeiro D, Matos M, et al. ANKH and susceptibility to and severity of ankylosing spondylitis. J Rheumatol. 2012; 39:131–134. [PubMed: 22089454]
40. Reveille JD, Sims AM, et al. Australo-Anglo-American Spondyloarthritis C. Genome-wide association study of ankylosing spondylitis identifies non-MHC susceptibility loci. Nat Genet. 2010; 42:123–127. [PubMed: 20062062]
41. Li G, Han N, Li Z, et al. Identification of transcription regulatory relationships in rheumatoid arthritis and osteoarthritis. Clin Rheumatol. 2013; 32:609–615. [PubMed: 23296645]
42. Simsa-Maziel S, Zaretsky J, Reich A, et al. IL-1RI participates in normal growth plate development and bone modeling. Am J Physiol Endocrinol Metab. 2013; 305:E15–E21. [PubMed: 23592480]
43. Sokolowska M, Chen LY, Eberlein M, et al. Low molecular weight hyaluronan activates cytosolic phospholipase A2alpha and eicosanoid production in monocytes and macrophages. J Biol Chem. 2014; 289:4470–4488. [PubMed: 24366870]
44. Kondo Y, Iizuka M, Wakamatsu E, et al. Overexpression of T-bet gene regulates murine autoimmune arthritis. Arthritis Rheum. 2012; 64:162–172. [PubMed: 21905017]
45. Aouadi M, Tesz GJ, Nicoloro SM, et al. Orally delivered siRNA targeting macrophage Map4k4 suppresses systemic inflammation. Nature. 2009; 458:1180–1184. [PubMed: 19407801]
46. Rouault K, Scotet V, Autret S, et al. Do HOXB9 and COL1A1 genes play a role in congenital dislocation of the hip? Study in a Caucasian population. Osteoarthritis Cartilage. 2009; 17:1099–1105. [PubMed: 19341834]
47. Blackstock CD, Higashi Y, Sukhanov S, et al. Insulin-like Growth Factor-1 Increases Synthesis of Collagen Type I via Induction of the mRNA-binding Protein LARP6 Expression and Binding to the 5' Stem-loop of COL1a1 and COL1a2 mRNA. J Biol Chem. 2014; 289:7264–7274. [PubMed: 24469459]
48. Schlondorff J, Blobel CP. Metalloprotease-disintegrins: modular proteins capable of promoting cell-cell interactions and triggering signals by protein-ectodomain shedding. J Cell Sci. 1999; 112(Pt 21):3603–3617. [PubMed: 10523497]
49. Jackson MT, Moradi B, Smith MM, et al. Matrix metalloproteinase (MMP)-2, MMP-9 and MMP-13 are activated by Activated Protein C (APC) in human osteoarthritic cartilage chondrocytes. Arthritis & rheumatology. 2014
50. Gill SE, Gharib SA, Bench EM, et al. Tissue inhibitor of metalloproteinases-3 moderates the proinflammatory status of macrophages. Am J Respir Cell Mol Biol. 2013; 49:768–777. [PubMed: 23742180]
51. Ciurtin C, Majeed Y, Naylor J, et al. TRPM3 channel stimulated by pregnenolone sulphate in synovial fibroblasts and negatively coupled to hyaluronan. BMC Musculoskelet Disord. 2010; 11:111. [PubMed: 20525329]

52. Jaeger K, Selent C, Jaehme W, et al. The genetics of osteoarthritis in STR/ort mice. Osteoarthritis Cartilage. 2008; 16:607–614. [PubMed: 17931911]

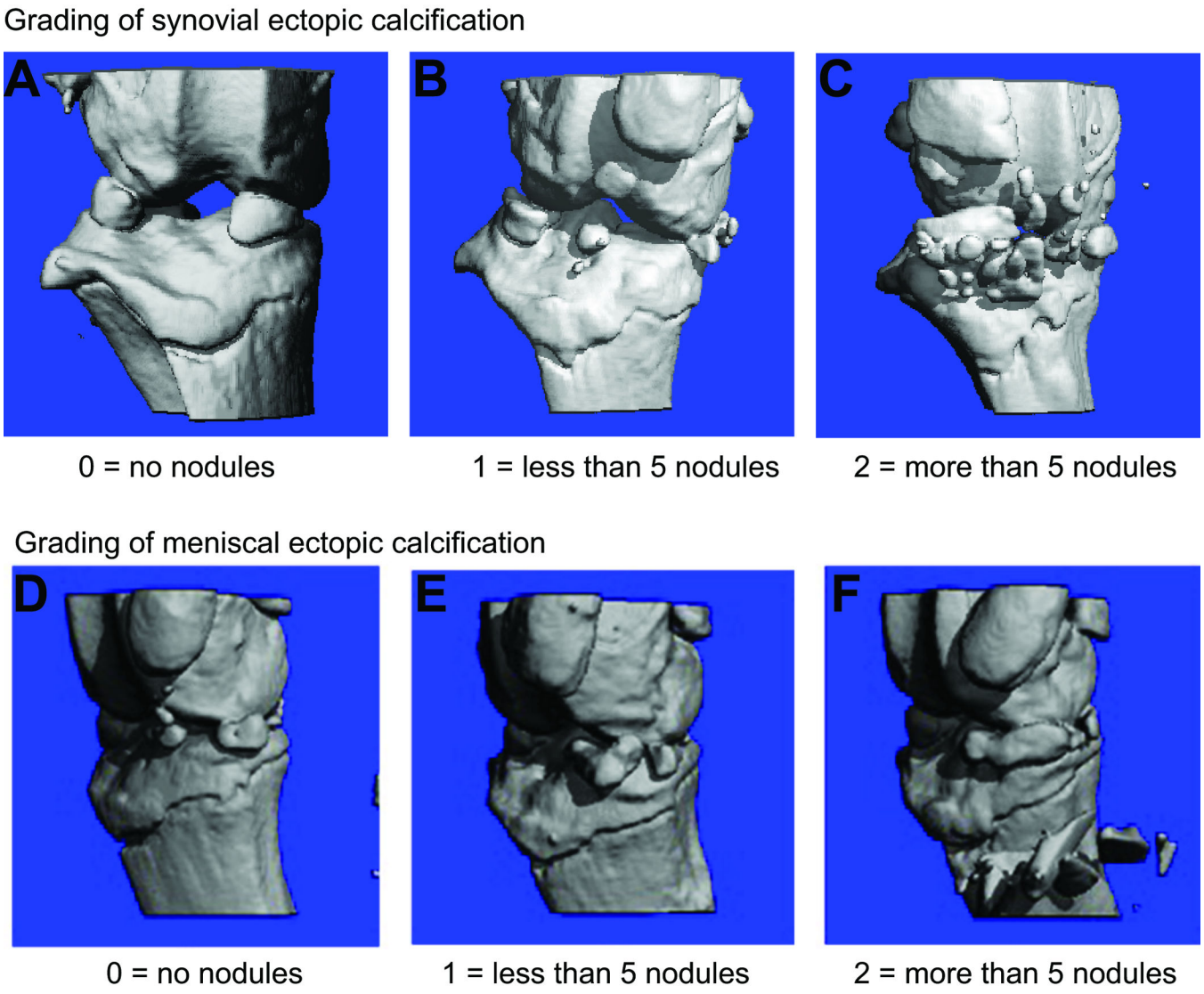

Fig. 1. Scoring scheme to evaluate ectopic calcification

We used binary and graded scoring schemes to evaluate the intensity of ectopic synovial (A–C) and meniscal (D–F) calcifications. Knees with no nodules were scored as absent (A, D) while knees with any calcification were scored as present (B, C, E, F) using binary scoring scheme. In the graded scheme 0 means no nodules (A, D), 1 means <5 nodules (B, E) and 2 means ≥5 nodules (C, F).

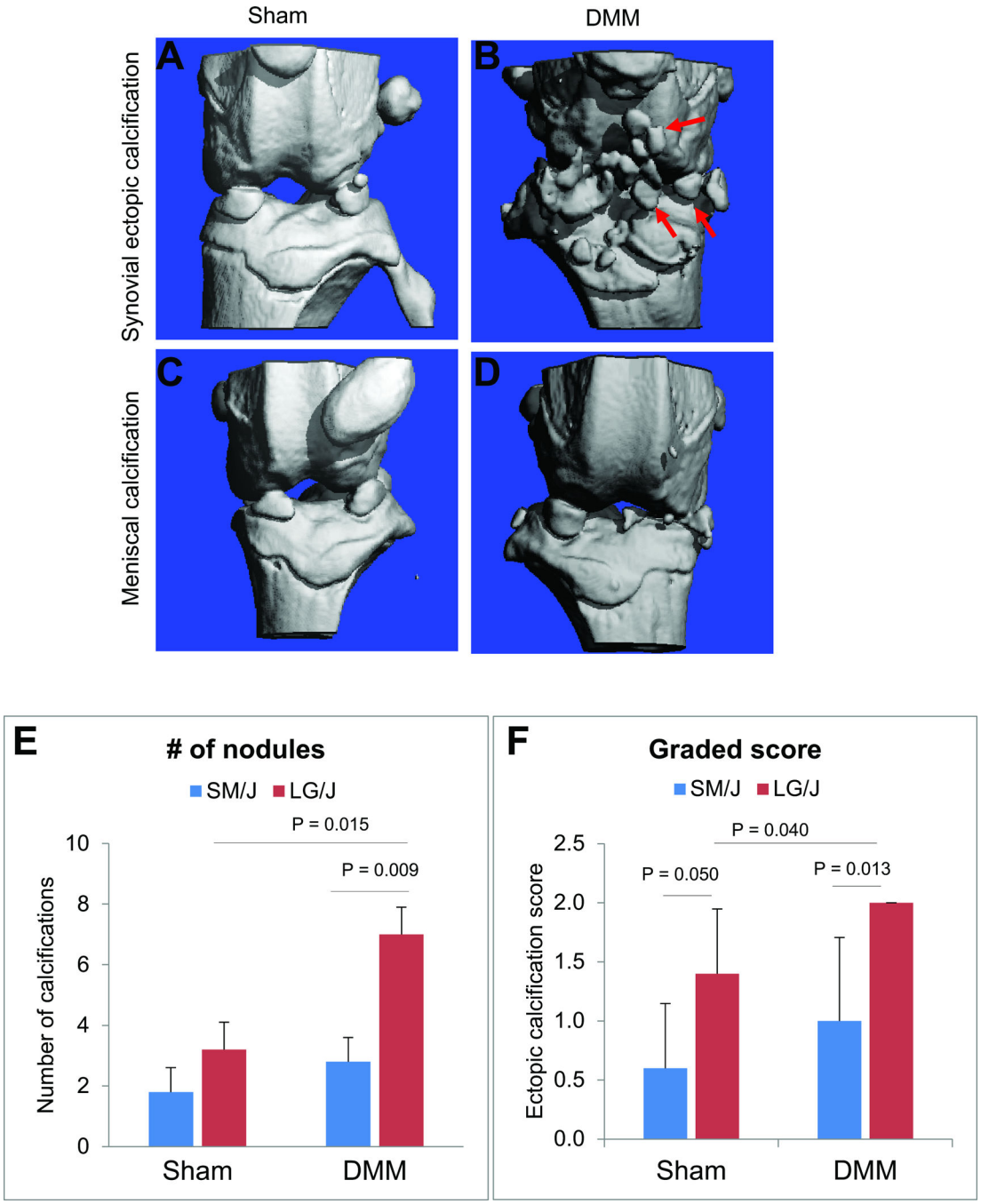

Fig. 2. Typical phenotypic outcomes in sham and DMM knees

F_{44} advanced intercross line mice were subjected to DMM at 10-week of age. Micro-CT analysis on the harvested knees was performed 8-week post-surgery. Micro-CT images showed ectopic synovial (A–B) and meniscal (C–D) calcifications exclusively in the knees subjected to DMM. No significant calcifications were observed in contralateral sham knees (A, C). We observed that ectopic synovial calcifications were significantly higher in the knees subjected to DMM of LG/J compared to contralateral sham-operated knee as well as DMM-operated knee of SM/J strain (E–F).

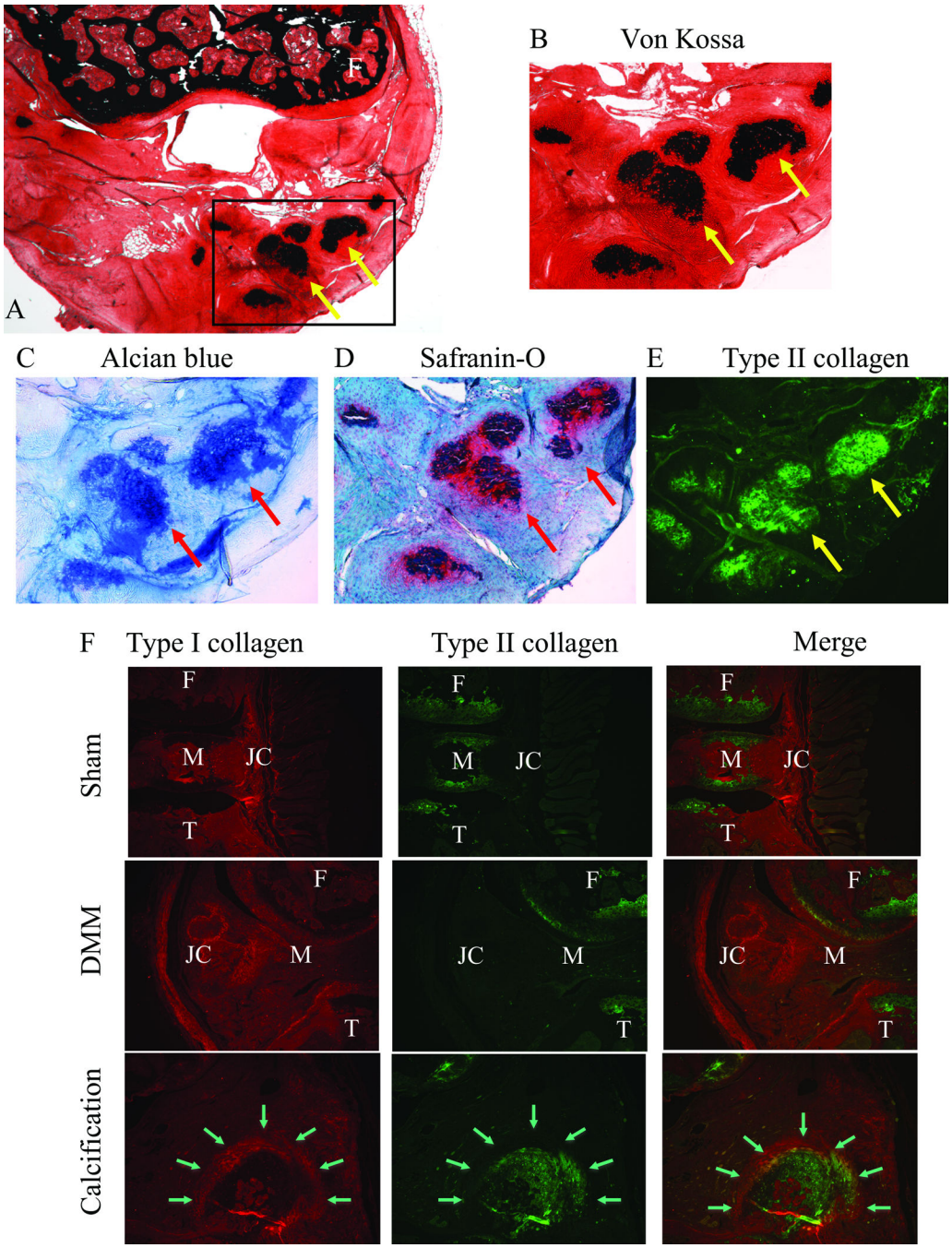

Fig. 3. Histological characteristics of ectopic calcifications

Lower magnification of anterior joint capsule stained with Von Kossa (A). Yellow arrows indicate ectopic calcification. High magnification of ectopic calcifications stained with von Kossa (B), Alcian blue (C), Safranin-O (D), and immunohistochemistry of type II collagen (E) are also shown. Immunohistochemistry of type I and II collagen on medial knee joint (sham and DMM) and ectopic calcification (arrows) are shown (F). F: Femur, M: Meniscus, T: Tibia, and JC: Joint capsule.

Table 1

Summary of quantitative trait loci and phenotypic effects.

QTL	Chr	Tissue	LPR	Peak Mbp[a]	Proximal Mbp	Distal Mbp	Interval length	Effects[b]	Sex	a/SD[c]	d/SD	i/SD	a SE[d]	d SE	i SE	Genes[e]
C1.1	1	synovium	3.99	38.746	38.094	38.932	0.838	a, as, ds	M	**−1.223**	−0.834	0.338	0.134	0.167	0.068	5
									F	0.028	0.548	−0.039	0.096	0.116	0.071	
C1.2	1	synovium	5.20	40.035	39.657	40.460	0.803	a, i, ds, is	M	**−0.478**	**−0.502**	0.004	0.054	0.076	0.046	6
									F	**−0.334**	0.139	**−0.393**	0.047	0.067	0.047	
C1.3	1	synovium	3.08	155.851	155.549	156.758	1.209	is	M	0.054	−0.102	**0.511**	0.052	0.088	0.050	7
									F	0.009	−0.084	**−0.334**	0.058	0.088	0.049	
C1.4	1	synovium	3.77	181.640	180.846	182.258	1.412	a, d, as	M	−0.131	0.114	−0.045	0.078	0.120	0.082	9
									F	**0.266**	−0.232	−0.227	0.079	0.102	0.062	
C1.5	1	meniscus	3.15	189.133	187.601	189.319	1.717	i	B	−0.158	**−0.269**	**−0.204**	0.042	0.058	0.037	6
C1.6	1	meniscus	3.06	192.193	191.851	192.530	0.679	a, d, as, ds	M	−0.069	−0.048	−0.186	0.075	0.111	0.056	1
									F	**−0.702**	**0.893**	−0.075	0.072	0.118	0.062	
C4.1	4	synovium	4.04	38.157	37.705	38.537	0.832	a, d, as, ds	M	0.025	0.079	0.006	0.047	0.063	0.044	0
									F	**−0.524**	**−0.379**	−0.072	0.037	0.052	0.039	
C5.1	5	meniscus	3.71	74.537	74.281	75.687	1.406	a, d	B	**0.589**	**0.477**	0.115	0.057	0.069	0.037	10
C5.2	5	meniscus	4.06	136.041	135.867	136.190	0.322	a, d, ds, is	M	0.175	0.120	**0.376**	0.127	0.256	0.123	6
									F	0.139	−1.142	**−0.128**	0.137	0.259	0.107	
C6.1	6	synovium	3.48	4.608	4.177	5.219	1.042	a, d	B	**−0.114**	**−0.152**	−0.006	0.021	0.028	0.019	8
C6.2	6	meniscus	3.17	61.571	59.615	63.355	3.740	i, is	M	−0.171	−0.203	**−0.428**	0.043	0.060	0.043	4
									F	0.017	0.148	0.016	0.052	0.070	0.051	
C8.1	8	meniscus	3.20	11.324	10.972	12.150	1.178	as, ds	M	**−0.625**	−0.365	0.001	0.185	0.209	0.121	10
									F	**0.331**	**0.709**	−0.218	0.153	0.201	0.129	
C9.1	9	synovium	3.25	61.044	60.553	61.490	0.936	d	B	−0.046	**−0.160**	0.011	0.021	0.031	0.022	3
C9.2	9	synovium	3.51	70.435	69.607	70.785	1.177	a	B	**0.128**	−0.075	−0.003	0.019	0.029	0.021	12
C10.1	10	meniscus	3.19	86.056	85.478	86.812	1.334	ds	M	0.183	**−0.469**	0.072	0.041	0.056	0.043	6
									F	−0.027	**0.345**	0.152	0.047	0.068	0.052	
C11.1	11	synovium	3.73	96.433	96.047	97.102	1.055	i, ds, is	M	0.180	−0.135	−0.111	0.045	0.065	0.046	28

QTL	Chr	Tissue	LPR	Peak Mbp[a]	Proximal Mbp	Distal Mbp	Interval length	Effects[b]	Sex	a/SD[c]	d/SD	i/SD	a SE[d]	d SE	i SE	Genes[e]
									F	0.051	0.291	**0.468**	0.044	0.062	0.044	
C13.1	13	synovium	3.20	32.496	32.257	33.510	1.253	a, d, i	B	**0.324**	**−0.237**	**0.163**	0.034	0.043	0.030	13
C14.1	14	meniscus	3.57	120.301	120.062	120.872	0.810	a, is	M	−0.292	−0.333	**−0.460**	0.069	0.095	0.053	3
									F	−0.514	−0.148	0.142	0.081	0.116	0.062	
C15.1	15	meniscus	3.51	27.470	27.316	27.624	0.307	d	B	−0.119	**0.761**	0.099	0.045	0.075	0.040	
C19.1	19	synovium	3.58	51.468	50.737	51.891	1.154	a, d	B	**0.308**	**−0.477**	−0.109	0.036	0.051	0.033	3
C19.1	19	meniscus	3.10	51.517	50.982	51.894	0.911	d, as, is	M	0.121	0.418	0.139	0.116	0.165	0.102	1
									F	**−0.332**	0.245	−0.213	0.114	0.159	0.101	

QTL = quantitative trait locus; LPR = -log (probability); a. Mbp = genome coordinates in millions of base pairs; b. a, d, i = additive, dominance, imprinting effects; as, ds, is = additive, dominance, imprinting by sex interaction effects; c. SD = standard deviation; c. SD = standard deviation; d. SE = standard error; e. number of known genes within interval; M = male, F = female, B = both (pooled sexes); The standardized effect sizes in boldface are statistically significant at ≤5% level

Table 2

Top 66 candidate genes based on SNP composition

				Total SNPs		Coding SNPs							Noncoding SNPs											
QTL	**tissue**	**Gene***	**RefGeneID**	**SNPs**	***HC*[a]**	**Total coding**	***HC***	***nsyn*[b]**	***HC***	***Prediction*[c]**	***syn*[d]**	***HC***	**Total noncoding**	***HC***	**2500 bp up stream**	***HC***	**5' UTR**	***HC***	**Introns**	***HC***	**3' UTR**	***HC***	**2500 bp down stream**	***HC***
C1.1	synovium	***Aff3***	NM_010678	587	16	6	2	2	0	.	4	2	581	14	0	0	0	0	557	14	2	0	22	0
		Lonrf2	NM_001029878	7	2	0	0	0	0	.	0	0	7	2	0	0	1	1	2	0	1	1	3	0
		Chst10	NM_145142	174	2	1	0	0	0	.	1	0	173	2	8	0	0	0	138	2	8	0	19	0
C1.2	synovium	*Rfx8*	NM_001145660	44	1	0	0	0	0	.	0	0	44	1	8	0	0	0	36	1	0	0	0	0
		Map4k4	NM_001252200	380	12	7	6	0	0	.	7	6	373	6	10	0	0	0	358	6	2	0	3	0
		Il1rl2	NM_133193	273	4	13	3	6	0	.	7	3	260	1	14	0	1	0	220	1	0	0	25	0
C1.3	synovium	*Teddm1*	NM_178244	1	1	0	0	0	0	.	0	0	1	1	0	0	0	0	1	1	0	0	0	0
		Zfp648	NM_001204908	1	0	1	0	1	0	.	0	0	0	0	0	0	0	0	0	0	0	0	0	0
C1.4	synovium	***Kif26b***	NM_001161665	368	7	0	0	0	0	.	0	0	368	7	0	0	0	0	368	7	0	0	0	0
		Smyd3	NM_027188	6	1	0	0	0	0	.	0	0	6	1	0	0	0	0	6	1	0	0	0	0
C1.5	meniscus	***Rrp15***	NM_026041	46	3	1	0	1	0	.	0	0	45	3	3	0	0	0	40	3	1	0	1	0
		D1Pas1	NM_033077	6	1	0	0	0	0	.	0	0	6	1	4	0	1	0	1	1	0	0	0	0
		Spata17	NM_028848	149	6	0	0	0	0	.	0	0	149	6	2	0	0	0	140	6	0	0	7	0
		Gpatch2	NM_026367	412	14	1	0	0	0	.	1	0	411	14	1	0	0	0	410	14	0	0	0	0
C1.6	meniscus	***Prox1***	NM_008937	99	7	1	0	0	0	.	1	0	98	7	5	0	0	0	91	6	0	0	2	1
C5.1	meniscus	***Rasl11b***	NM_026878	26	4	3	2	0	0	.	3	2	23	2	12	0	1	0	6	2	0	0	4	0
		Scfd2	NM_001114660	492	7	0	0	0	0	.	0	0	492	7	0	0	0	0	456	7	10	0	26	0
		Fip1l1	NM_001159573	40	1	0	0	0	0	.	0	0	40	1	0	0	0	0	34	1	2	0	4	0
		Lnx1	NM_001159578	376	4	3	1	0	0	.	3	1	375	3	9	0	1	0	356	3	7	0	2	0
C5.2	meniscus	*Pom121*	NM_148932	1	1	0	0	0	0	.	0	0	1	1	0	0	0	0	0	0	0	0	1	1
		Hip1	NM_146001	23	0	2	0	1	0	.	1	0	21	0	1	0	0	0	20	0	0	0	0	0
		Ccl26	NM_001013412	8	3	1	1	0	0	.	0	0	7	2	2	0	1	1	2	0	1	1	1	0
C6.1	synovium	*Casd1*	NM_145398	19	1	0	0	0	0	.	0	0	19	1	2	1	0	0	15	0	0	0	2	0
		Sgce	NM_001130190	99	5	0	0	0	0	.	0	0	99	5	2	0	0	0	89	5	4	0	4	0
		Ppp1r9a	NM_181595	48	1	0	0	0	0	.	0	0	48	1	3	0	0	0	38	1	6	0	1	0

				Total SNPs		Coding SNPs							Noncoding SNPs											
QTL	**tissue**	**Gene***	**RefGeneID**	**SNPs**	***HC*[a]**	**Total coding**	***HC***	***nsyn*[b]**	***HC***	***Prediction*[c]**	***syn*[d]**	***HC***	**Total noncoding**	***HC***	**2500 bp up stream**	***HC***	**5' UTR**	***HC***	**Introns**	***HC***	**3' UTR**	***HC***	**2500 bp down stream**	***HC***
		Pon1	NM_011134	130	5	3	1	0	0	.	3	1	127	4	0	0	0	0	126	4	0	0	1	0
		Pon2	NM_183308	62	4	3	3	0	0	.	3	3	59	1	5	0	0	0	49	1	2	0	3	0
C6.2	meniscus	***Grid2***	NM_008167	1556	17	2	1	0	0	.	2	1	1554	16	0	0	1	1	1552	15	0	0	1	0
C8.1	meniscus	*Irs2*	NM_001081212	3	3	1	1	0	0	.	0	0	2	2	0	0	1	1	0	0	1	1	0	0
		Col4a2	NM_009932	637	11	23	10	3	0	.	20	10	614	1	0	0	0	0	604	1	5	0	5	0
		Rab20	NM_011227	241	4	3	1	1	0	.	2	1	238	3	25	0	1	1	197	1	1	1	14	0
		Carkd	NM_001190357	198	0	2	0	1	0	.	1	0	196	0	32	0	2	0	135	0	3	0	24	0
		Cars2	NM_024248	405	0	6	0	2	0	.	4	0	399	0	24	0	1	0	347	0	0	0	27	0
		Ankrd10	NM_001281975	149	7	2	1	1	1	.	1	0	147	6	16	0	1	1	115	5	0	0	15	0
C9.1	synovium	***Uaca***	NM_028283	235	5	20	4	3	0	.	17	4	215	1	1	0	0	0	198	0	0	0	16	1
		Tle3	NM_001083927	46	4	3	2	0	0	.	3	2	43	2	1	0	0	0	33	2	3	0	6	0
C9.2	synovium	*Fam81a*	NM_029784	109	2	0	0	0	0	.	0	0	109	2	7	0	0	0	101	2	0	0	1	0
		Myo1e	NM_181072	513	15	7	5	1	1	.	6	4	506	10	0	0	0	0	502	10	2	0	2	0
		Fam63b	NM_172772	5	1	1	1	1	1	LRT	0	0	4	0	0	0	0	0	3	0	1	0	0	0
		Adam10	NM_007399	9	1	0	0	0	0	.	0	0	9	1	0	0	0	0	9	1	0	0	0	0
C10.1	meniscus	*Syn3*	NM_013722	687	14	3	1	0	0	.	3	1	684	13	0	0	0	0	635	13	47	0	2	0
		Timp3	NM_011595	139	6	2	2	0	0	.	2	2	137	4	26	0	0	0	104	4	4	0	3	0
		Stab2	NM_138673	826	5	25	3	14	1	LRT	11	2	801	2	37	0	0	0	762	2	0	0	2	0
C11.1	synovium	*Hoxb9*	NM_008270	18	5	0	0	0	0	.	0	0	18	5	6	0	0	0	3	2	1	0	8	3
		Skap1	NM_001033186	2063	160	7	4	3	1	Polyphen2	4	3	2056	156	0	0	0	0	1960	156	62	0	34	0
		Snx11	NM_001163389	60	2	3	1	2	1	.	1	0	57	1	8	0	0	0	36	0	4	0	9	1
		Cbx1	NM_007622	108	4	0	0	0	0	.	0	0	108	4	15	0	1	0	78	4	2	0	12	0
		Nfe2l1	NM_001130450	66	9	3	3	0	0	.	3	3	63	6	19	2	0	0	20	3	3	0	21	1
		Copz2	NM_019877	164	3	1	1	0	0	.	1	1	163	2	28	0	0	0	112	2	3	0	20	0
		Cdk5rap3	NM_030248	93	6	9	4	3	1	.	6	3	84	2	15	0	0	0	50	0	4	0	15	2
		Pnpo	NM_134021	70	2	2	1	1	0	.	1	1	68	1	22	1	0	0	21	0	10	0	15	0
		Sp2	NM_001080964	123	6	5	5	0	0	.	5	5	118	1	7	0	0	0	89	1	4	0	18	0
		Sp6	NM_031183	68	3	1	0	0	0	.	1	0	67	3	14	2	0	0	36	1	5	0	12	0

				Total SNPs		Coding SNPs							Noncoding SNPs										
QTL	**tissue**	**Gene***	**RefGeneID**	**SNPs**	***HC*[a]**	**Total coding**	***HC***	***nsyn*[b]**	***HC***	***Prediction*[c]**	***syn*[d]**	***HC***	**Total noncoding**	***HC***	**2500 bp up stream**	***HC***	**5' UTR**	***HC***	**Introns**	***HC***	**3' UTR**	***HC***	**2500 bp down stream**	***HC***
		Scrn2	NM_146027	37	3	6	2	2	0	.	4	2	31	1	8	0	0	0	7	0	0	0	16	1
		Lrrc46	NM_027026	70	5	5	1	2	0	.	3	1	65	4	15	0	2	0	32	2	1	0	15	2
		Mrpl10	NM_026154	93	4	5	3	2	1	.	3	2	88	1	15	0	0	0	50	0	12	0	11	1
		Osbpl7	NM_001081434	181	10	12	10	1	0	.	11	10	169	0	20	0	1	0	126	0	2	0	20	0
		Tbx21	NM_019507	74	4	4	2	0	0	.	4	2	70	2	0	0	0	0	46	2	7	0	17	0
C13.1	synovium	***Gmds***	NM_146041	81	2	0	0	0	0	.	0	0	81	2	1	0	0	0	79	2	0	0	1	0
C14.1	meniscus	*Hs6st3*	NM_015820	844	25	1	0	0	0	.	1	0	843	25	0	0	0	0	843	25	0	0	0	0
		Oxgr1	NM_001001490	48	2	5	2	3	2	LRT; SIFT	2	0	43	0	7	0	0	0	32	0	1	0	3	0
		Mbnl2	NM_175341	691	27	2	2	0	0	.	2	2	689	25	0	0	1	0	668	25	1	0	19	0
C15.1	meniscus	*Ank*	NM_020332	520	2	3	2	0	0	.	3	2	519	1	2	0	0	0	513	1	2	0	2	0
		Fam105b	NM_001013792	82	2	0	0	0	0	.	0	0	81	1	33	0	0	0	47	1	0	0	1	0
		Fam105a	NM_001242424	254	3	6	2	3	0	LRT; Polyphen2	3	2	253	2	0	0	0	0	187	2	25	0	41	0
C19.1	meniscus/synovium	***Sorcs1***	NM_001252501	1885	48	4	0	2	0	.	2	0	1881	48	10	0	0	0	1841	48	10	0	20	0

QTL = quantitative trait locus; SNP = single nucleotide polymorphism; a. Highly conserved; b. nonsynonymous; c. LRT, SIFT, and/or PolyPhen-2 algorithm predictions of SNP; d. synonymous; Top nominated genes based on SNP composition and algorithm per interval are in boldface.

Table 3

Gene transcripts significantly differentially expressed between parental LG/J and SM/J inbred mouse strains

Chromosome	Gene	LG/J	SM/J	P value	Standard error	QTL interval	HC noncoding SNPs	correlation with calcification	P value
1	*Aff3*	0.048	−0.055	0.03	0.038	C1.1	14	0.56	0.02*
1	*Gpatch2*	0.008	−0.101	0.07	0.053	C1.5	14	0.39	0.11
6	*Pon2*	0.021	−0.054	0.06	0.036	C6.1	1	0.38	0.12
9	*Uaca*	0.019	−0.087	0.10	0.059	C9.1	1	0.18	0.48
9	*Fam81a*	0.057	−0.061	0.02	0.039	C9.2	2	0.46	0.06*
10	*Syn3*	0.092	−0.018	0.03	0.040	C10.1	13	0.43	0.08*
11	*Copz2*	0.075	−0.052	0.07	0.061	C11.1	2	−0.27	0.26
11	*Skap1*	0.073	−0.040	0.03	0.043	C11.1	156	0.17	0.51
11	*Mrpl10*	0.036	−0.055	0.04	0.035	C11.1	1	−0.14	0.58
11	*Nfe2l1*	0.035	−0.078	0.05	0.046	C11.1	6	−0.28	0.27
15	*Ank*	0.084	−0.017	0.09	0.050	C15.1	1	0.40	0.10*

QTL = quantitative trait locus; HC = highly conserved; SNP = single nucleotide polymorphism